ELL, a novel TFIIH partner, is involved in transcription restart after DNA repair

Sophie Mourgues[a,b], Violette Gautier[a,b], Anna Lagarou[a,b], Christine Bordier[a,b], Amandine Mourcet[a,b], Joris Slingerland[a,b], Lara Kaddoum[a,b], Frédéric Coin[c], Wim Vermeulen[d], Anne Gonzales de Peredo[a,b], Bernard Monsarrat[a,b], Pierre-Olivier Mari[a,b,1], and Giuseppina Giglia-Mari[a,b,1,2]

[a]Institut de Pharmacologie et de Biologie Structurale, Centre National de la Recherche Scientifique, F-31077 Toulouse, France; [b]Institut de Pharmacologie et de Biologie Structurale, Université Paul Sabatier, Université de Toulouse, F-31077 Toulouse, France; [c]Department of Functional Genomics, Institut de Génétique et de Biologie Moléculaire et Cellulaire, Institut National de la Santé et de la Recherche Médicale, Université Louis Pasteur, Centre National de la Recherche Scientifique, 67400 Illkirch Graffenstaden, France; and [d]Department of Genetics, Erasmus University Medical Center, Rotterdam, The Netherlands

Edited by Philip C. Hanawalt, Stanford University, Stanford, CA, and approved September 19, 2013 (received for review March 14, 2013)

DNA lesions that block transcription may cause cell death even when repaired, if transcription does not restart to reestablish cellular metabolism. However, transcription resumption after individual DNA-lesion repair remains poorly described in mechanistic terms and its players are largely unknown. The general transcription factor II H (TFIIH) is a major actor of both nucleotide excision repair subpathways of which transcription-coupled repair highlights the interplay between DNA repair and transcription. Using an unbiased proteomic approach, we have identified the protein eleven-nineteen lysine-rich leukemia (ELL) as a TFIIH partner. Here we show that ELL is recruited to UV-damaged chromatin in a Cdk7- dependent manner (a component of the cyclin-dependent activating kinase subcomplex of TFIIH). We demonstrate that depletion of ELL strongly hinders RNA polymerase II (RNA Pol II) transcription resumption after lesion removal and DNA gap filling. Lack of ELL was also observed to increase RNA Pol II retention to the chromatin during this process. Identifying ELL as an essential player for RNA Pol II restart during cellular DNA damage response opens the way to obtaining a mechanistic description of transcription resumption after DNA repair.

elongation factor | CAK | LEC | Cockayne syndrome | TCR

Damage to DNA induced by UV irradiation is repaired by the nucleotide excision repair (NER) system. Three DNA repair-deficient disorders emphasize the importance of NER in genome stability (1). In eukaryotic cells, NER can be divided into two pathways: global genome repair (GGR), repairing lesions throughout the genome, and transcription-coupled repair (TCR), which repairs lesions on the transcribed strand of active genes (2). After damage detection, the basal transcription/repair factor II H (TFIIH), containing the XPB and XPD ATPase/helicases is needed to locally unwind the DNA double helix around the lesion. Furthermore, in vitro UV irradiation elicits a change in the composition of TFIIH. Indeed the majority of TFIIH present on UV-damaged chromatin does not contain the ternary cyclin-dependent activating kinase (CAK) complex (3). More specifically, the CAK complex is found to be only implicated in TCR but not during GGR, where it seems to be released from the remaining TFIIH components, concomitantly with the recruitment of subsequent NER factors (3). To better our understanding of TFIIH functions in vivo, we have used a combination of improved immunoprecipitation assays and proteomic analysis to identify and characterize TFIIH-interacting partners.

Our quantitative proteomic approach has identified several putative TFIIH partners, of which the four most enriched constitute the Little Elongation Complex (LEC): eleven-nineteen lysine-rich leukemia (ELL), EAF1 (ELL-associated factor 1), KIAA0947, and NARG2 (4). The proposed role of the LEC is to regulate the transcription of small nuclear RNA genes (5). Although ELL and EAF1 are also part of the Super Elongation Complex (SEC), known to regulate the transcriptional elongation checkpoint control (important for gene expression regulation during development) (6–8), we focused this study on the LEC, because none of the other SEC components were identified. In the present study, we have discovered an unexpected role for ELL during DNA damage response. Specifically, our data show that ELL is essential for transcription resumption after removal of transcription blocking DNA lesions by the TCR machinery.

Results

Identification of Unique TFIIH Partners. To efficiently immunopurify the TFIIH complex and associated protein partners for proteomic analysis, we used ES cells isolated from a knock-in mouse endogenously expressing a YFP-tagged XPB helicase (9). Only the XPB–YFP version of the protein is expressed in the mouse cells and its expression is driven by the endogenous XPB promoter. A quantitative proteomic approach (10) was applied to compare immunopurified complexes and identify proteins specifically interacting with TFIIH. In our analysis, all 10 TFIIH subunits (the 7 "core" components XPB, XPD, p62, p52, p44, p34, and TTDA, together with the ternary CAK subcomplex composed of Cdk7, Mat1, and cyclin H) were identified together with the XPG endonuclease (11). Interestingly, among the small group of highly specific TFIIH-interacting partners, we identified the four proteins (ELL, EAF1, KIAA0947, and NARG2) composing the LEC (Fig. 1*A* and *SI Appendix*, Table S1).

To determine which TFIIH component interacts with the LEC, we chose to investigate ELL, the highest-ranking LEC component of our list (Fig. 1*A*, *Inset*). First, immunoblotting

Significance

A variety of genotoxic agents cause DNA lesions which, when located on a transcribed gene, will block the RNA polymerase II and recruit DNA repair proteins, including the basal transcription factor IIH, to restore the genetic information via the pathway known as transcription-coupled repair. Once the repair process is completed, transcription is expected to restart to restore proper cellular functions. RNA polymerase II restart after DNA repair in higher eukaryotes has not been studied mechanistically. We have identified eleven-nineteen lysine-rich leukemia as specifically involved in transcription resumption after DNA repair and have been able to measure the effect of its absence on transcription and the dynamic behavior of RNA polymerase II during transcription-coupled repair.

Author contributions: S.M., P.-O.M., and G.G.-M. designed research; S.M., V.G., A.L., C.B., A.M., J.S., L.K., F.C., A.G.d.P., and P.-O.M. performed research; W.V. contributed new reagents/analytic tools; S.M., V.G., A.G.d.P., B.M., P.-O.M., and G.G.-M. analyzed data; and S.M., P.-O.M., and G.G.-M. wrote the paper.

The authors declare no conflict of interest.

This article is a PNAS Direct Submission.

[1]P.-O.M. and G.G.-M. contributed equally to this work.

[2]To whom correspondence should be addressed. E-mail: mari@ipbs.fr.

This article contains supporting information online at www.pnas.org/lookup/suppl/doi:10.1073/pnas.1305009110/-/DCSupplemental.

using a polyclonal antibody raised against ELL confirmed that this 68-kDa polypeptide copurified with TFIIH (Fig. 1*B*). Then, recombinant TFIIH subunits were tested for their interaction with the bacterially produced and purified GST–ELL polypeptide. Although recombinant GST–ELL was able to pull down the whole in vitro reconstituted TFIIH complex (Fig. 1*C*), when TFIIH subunits were individually tested, Cdk7 was the only one specifically pulled down with GST–ELL (Fig. 1*D* and *SI Appendix*, Fig. S1).

To further examine the interaction between TFIIH and the LEC in living cells, we used a variant of fluorescence recovery after photobleaching (FRAP) assay (12, 13) to compare the dynamic behavior of ELL–GFP to XPB–GFP (13) (a core TFIIH factor) and Cdk7 (CAK subunit). Our FRAP data show that ELL–GFP mobility is much higher than the mobility of XPB–GFP and similar to that of Cdk7–GFP (Fig.1*E*). Although the nucleoplasm is not a homogenous medium, a clear relationship exists between molecular weight and diffusion speed (14, 15). The fact that Cdk7 (~40 kDa alone, ~110 kDa within the CAK) diffuses much faster than XPB indicates that these proteins diffuse in the nucleus separately, but at the same time does not exclude that a fraction of these proteins are part of the same, much larger, complex, that is, TFIIH (>500 kDa) (15). Conversely, although ELL is a known component of the SEC and LEC (both >350 kDa) (8), its fast mobility (comparable to Cdk7) indicates that ELL must also exist outside of these two large complexes (e.g., alone, together with EAF1, or in another small complex).

LEC Behavior During DNA Repair. Linking the LEC to TFIIH, via the ELL/Cdk7 interaction, prompted us to investigate the possible implication of the LEC in the DNA damage response. Strip-FRAP applied to UV-irradiated cells stably expressing GFP-tagged XPB, Cdk7, ELL, and EAF1 revealed an incomplete fluorescence recovery (or immobile fraction) except for EAF1–GFP (Fig. 2 *A*–*D*). This observed immobilization strongly suggests that ELL, but not EAF1, participates in the UV-induced DNA damage response. The immobile fractions measured for ELL–GFP and Cdk7–GFP were significantly smaller compared with that of XPB–GFP (Fig. 2 *A*–*C*). XPB–GFP, representing the core TFIIH, is involved in both GGR and TCR pathways, whereas Cdk7–GFP, representing the CAK subcomplex, is only targeted to the far less numerous TCR sites (3, 16, 17). Hence, our data suggest that ELL–GFP's response to DNA damage might be related to TCR. Additionally, ELL–GFP's UV-induced immobile fraction becomes undetectable after Cdk7 knockdown (Fig. 2*E*), suggesting that the ELL/Cdk7 interaction may serve to recruit ELL to the UV-damaged chromatin.

To further determine the nature of ELL's engagements during DNA damage response, we compared the recruitment speeds and levels of ELL, Cdk7, XPB, and the TCR-specific protein CSA (18) to locally microirradiated areas within living cell nuclei (Fig. 2 *F* and *G*) (17, 19). The progressive recruitment of XPB to

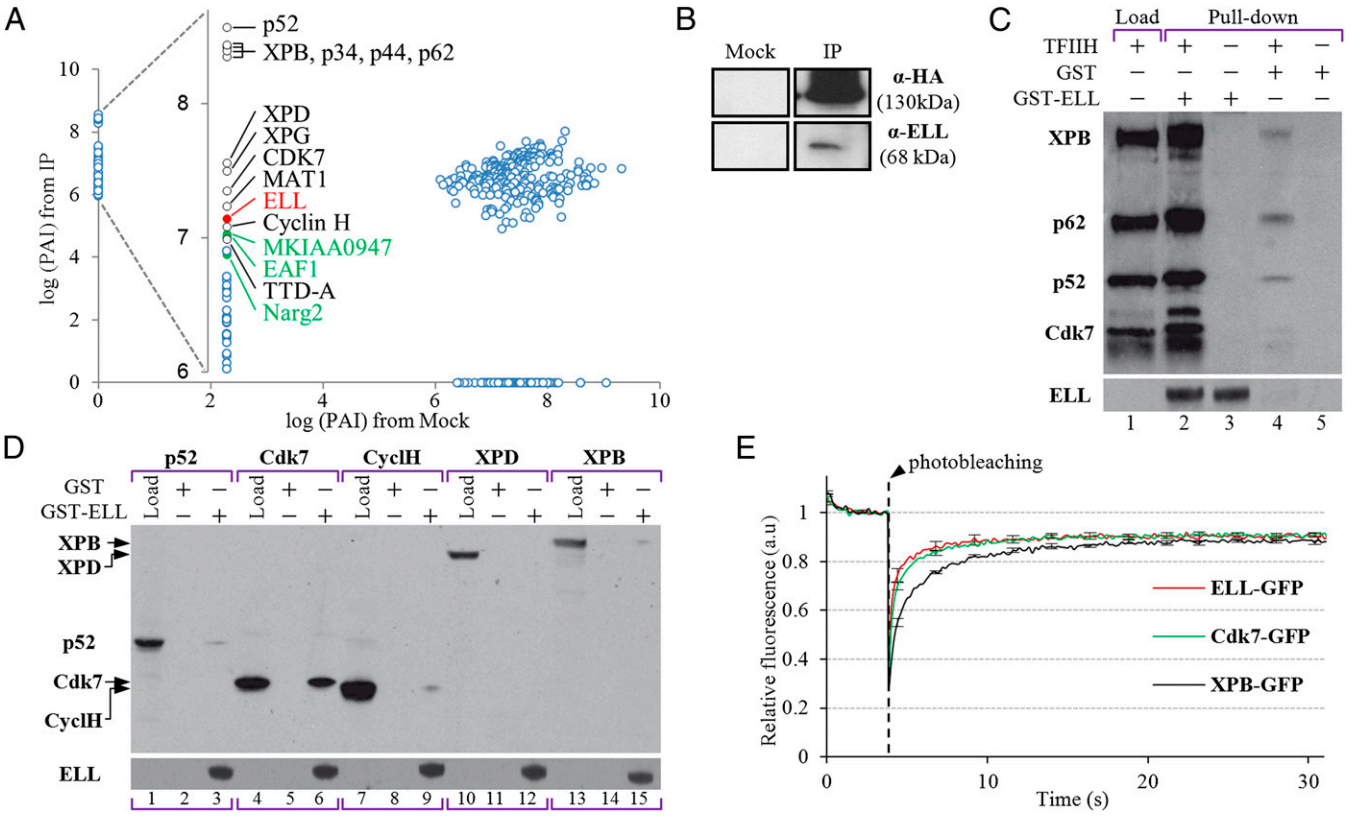

Fig. 1. Identification of interacting partners of TFIIH. (*A*) Quantitative proteomic analysis of proteins coimmunoprecipitated with XPB versus control sample. Data analysis was performed by plotting the log of a protein abundance index (PAI) derived from mass spectrometry signal intensity measurement. In four independent experiments, all TFIIH subunits as well as the LEC components ELL, MKIAA0947, EAF1, and NARG2 were specifically detected in the immunopurified complex. (*B*) Western blot showing a stable association between TFIIH and ELL in XPB–YFP-expressing ES cells. The immunoprecipitate was analyzed by Western blotting for HA and ELL antibodies. (*C*) Bacterially expressed TFIIH subunits were tested for their ability to interact with GST-tagged ELL (lane 2) or GST alone (lane 4) coupled to glutathione-agarose beads. Proteins on the resin were resolved by SDS/PAGE and immunostained. (*D*) SDS/PAGE analysis showing purified TFIIH subunits (lanes 1, 4, 7, 10, and 13), purified pulldown GST (lanes 2, 5, 8, 11, and 14), and pulldown GST–ELL (lanes 3, 6, 9, 12, and 15). Cdk7 is the only subunit of TFIIH interacting with ELL (*SI Appendix*, Fig. S1). (*E*) Normalized FRAP data measured in human fibroblasts stably expressing ELL–GFP (red), Cdk7–GFP (green), and XPB–GFP (black). Error bars represent SEM obtained from 15 cells.

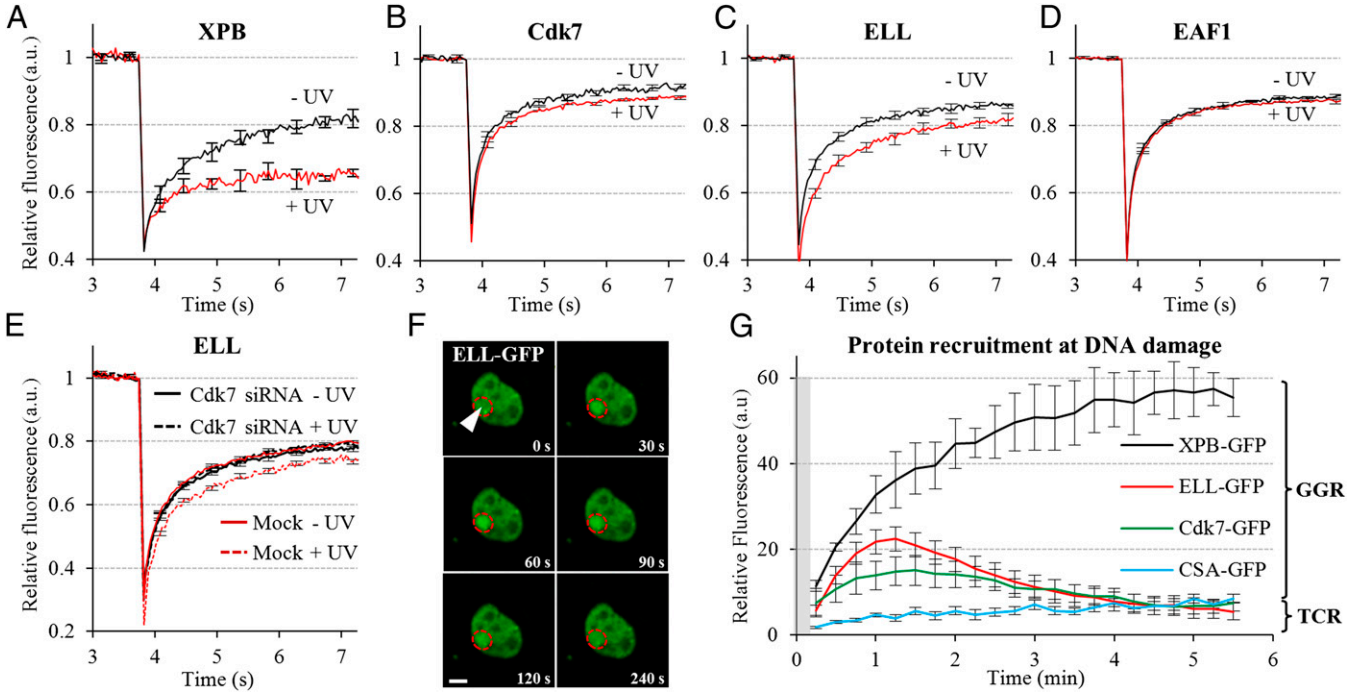

Fig. 2. ELL dynamics during DNA damage response. (*A–D*) FRAP curves plotted for XPB–GFP-, Cdk7–GFP-, ELL–GFP-, and EAF1–GFP-expressing cells treated (red) or not (black) with UV-C. (*E*) FRAP curves for ELL–GFP-expressing cells treated (black) or not (red) with siRNA against Cdk7, exposed (dashed lines) or not (solid lines) to UV. (*F*) Confocal time-lapse images of a living mammalian fibroblast expressing ELL–GFP, seen accumulating at a microirradiated area (arrow). (*G*) Accumulation curves of XPB–GFP, ELL–GFP, Cdk7–GFP, and CSA–GFP proteins at laser-induced DNA damage. Hatched region indicates time window during which microirradiation-induced photobleaching masks the accumulation signal. Error bars represent the SEM obtained from at least 10 cells.

the damaged area (Fig. 2*G*, black curve) is typical of early GGR pathway factors (20). As expected, the recruitment level of CSA is very weak (Fig. 2*G*, blue curve). Indeed, within the laser-targeted area, the total number of laser-induced UV lesions that will be repaired via GGR far exceeds the number of UV lesions that must be on the transcribed strand of active genes to be repaired by the TCR pathway (17, 19). The similar, yet atypical, recruitment curves of ELL and Cdk7 (Fig. 2*G*, red and green curves) show an initial rise followed by a slower drop with stabilization at a low level similar to what we measured for CSA. This result may indicate that a fraction of the TFIIH complexes recruited to GGR-processed DNA lesions initially contain the CAK, although it is not needed during GGR (3). Rapid release of the CAK in all but the TCR-processed lesions would then explain the fast drop and stabilization of its recruitment curve. Taken together, our results, showing that the dynamics of ELL and Cdk7 after UV exposure are similar, further support the idea that ELL (possibly without EAF1) could be involved in the TCR pathway.

ELL Is Involved in TCR. Because TFIIH mutants are UV-sensitive, we questioned whether ELL knockdown would have an effect on cell survival after UV irradiation. Repressing ELL expression by siRNA in normal human fibroblasts (*SI Appendix*, Fig. S2 and Table S2) led to a moderate UV-specific cytotoxicity, as measured by clonogenic survival (Fig. 3*A* and *SI Appendix*, Fig. S3). The ELL siRNA survival curve (Fig. 3*A*, red curve) was very similar to the one obtained for Cdk7 knockdown (Fig. 3*A*, green curve), whereas the knockdown of the well-known NER endonuclease XPF produced more severe UV cytotoxicity, as expected (Fig. 3*A*, purple curve). This result clearly indicates a specific role in NER for both ELL and the classic CAK factor Cdk7 (21).

To further dissect the involvement of ELL and Cdk7 during NER, we used two different assays that predominantly measure either GGR or TCR activity when applied to UV-irradiated cells: unscheduled DNA synthesis (UDS) and recovery of RNA synthesis (RRS), respectively. Incorporating a fluorophore-coupled deoxynucleoside analog to visualize newly synthesized DNA (22), the UDS assay allowed us to quantify DNA replication after repair (i.e., the refilling of single-strand DNA gaps generated by NER processing of UV-induced DNA lesions). We compared the UDS levels of UV-exposed ELL-, Cdk7-, and XPF-depleted cells to mock treated cells (Fig. 3*B*). XPF siRNA-treated cells showed a strong reduction in UDS levels compared with proficient cells (Fig. 3*B*, purple and black bars), as expected for NER-deficient cells unable to process UV lesions. However, ELL- and Cdk7-depleted cells showed no significant drop in UDS levels, suggesting that ELL and Cdk7 are not essential factors during GGR (Fig. 3*B*, red and green bars). In accordance with these results, using an in vitro repair assay (23) we also showed that TFIIH can support repair even in the absence of purified ELL (*SI Appendix*, Fig. S4).

Using the RRS assay, we then quantified TCR activity in globally UV-irradiated siRNA-treated cells by visualizing newly synthesized RNA after DNA repair (via a fluorophore-coupled nucleoside analog). Knockdown of ELL, Cdk7, and XPF (Fig. 3 *C* and *D*), but not EAF1, KIAA0947, NARG2 (*SI Appendix*, Fig. S5), or a murine ELL (human siRNA-resistant, *SI Appendix*, Fig. S7), resulted in a large reduction of RNA synthesis after UV. To test whether such reductions were DNA repair-specific, we repeated the RRS assay after localized UV exposure and found irradiation area-specific reductions of transcription in ELL, Cdk7, and XPF knockdown cells (*SI Appendix*, Fig. S10). Controlling whether transcription levels were not trivially reduced in these siRNA-treated cells (*SI Appendix*, Fig. S6) showed that only NARG2 knockdown had a mild effect (dark brown bar, *SI Appendix*, Figs. S5 and S6). Together, these data show that ELL, like Cdk7, is specifically involved in TCR, either directly during the repair of the transcription blocking DNA lesions or in the restart of transcription after completion of the repair process.

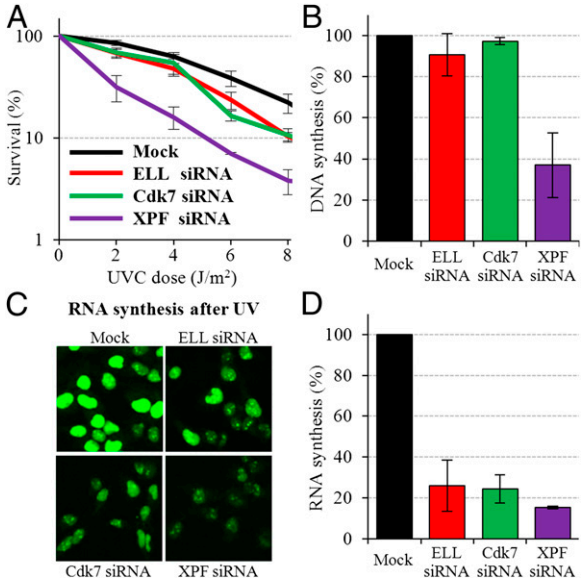

Fig. 3. Clonogenicity, UDS, and RRS of ELL-depleted cells. (*A*) Sensitivity to UV-C of immortalized human fibroblast MRC5 cells treated with siRNA against the indicated factors as determined by colony-forming ability (mean ± SEM): mock siRNA (black), ELL siRNA (red), Cdk7 siRNA (green), and XPF siRNA (purple). (*B*) UDS determined by EdU incorporation after UV-C exposure in MRC5 cells after siRNA against indicated factors. At least 100 nuclei were analyzed in three independent experiments; error bars represent the SEM. (*C*) Representative images of MRC5 cells analyzed in *D* showing recovery or inhibition of RNA synthesis following UV (shown in green via EdU incorporation), after mock or siRNA-mediated knockdown of the indicated factors. All images were captured using the same settings. (*D*) RRS after UV-C exposure in MRC5 cells with siRNA-mediated knockdown of the indicated factors. At least 100 nuclei were analyzed in three independent experiments; error bars represent the SEM.

ELL Is Essential for Transcription Resumption After Repair. To discriminate whether ELL plays a role in either the repair process or the restart of transcription after repair, we designed an assay to specifically measure repair replication during TCR (TCR-UDS). We used GGR-deficient XPC-negative cells to ensure that, within locally UV-exposed cell nuclei, repair replication was exclusively due to ongoing TCR. In combination with γ-H2AX immunofluorescence labeling (17, 24, 25) for precise localization of UV-induced DNA-damaged areas, we quantified repair replication in those areas via incorporation of a fluorophore-coupled deoxynucleoside analog into newly synthesized DNA (22) (Fig. 4*A* and *SI Appendix*, Fig. S8). With this assay we were able to monitor TCR-specific repair replication levels in cells depleted of ELL, Cdk7, XPF, or the TCR coupling factor CSB (26) (Fig. 4 *A* and *B*). As expected, because both GGR and TCR pathways are compromised in XPC-negative cells treated with siRNA against XPF or CSB, a low TCR-UDS was observed (Fig. 4*B*, purple and blue bars). Surprisingly, whereas Cdk7 knockdown also showed a TCR-UDS reduction comparable to XPF and CSB knockdown (Fig. 4*B*, green bar), treatment of XPC-negative cells with siRNA against ELL led to a normal TCR-UDS level (Fig. 4*B*, red bar). This result clearly indicates that depletion of ELL does not hinder UV-lesion processing by the TCR reaction.

Combining TCR-UDS with classic RRS (Fig. 3*D*) provided us with the opportunity to differentiate the repair reaction from transcription resumption after repair. Indeed, the very low RRS and reduced TCR-UDS following UV irradiation in knockdown Cdk7 cells demonstrate the requirement of the Cdk7 kinase in the repair process during TCR in vivo. Conversely, the low RRS but unchanged TCR-UDS levels in knockdown ELL cells suggests a molecular scenario in which ELL is not directly involved during the repair reaction but would have a specific role in RNA polymerase II (RNA Pol II) transcription resumption after individual UV-lesion repair.

To determine whether ELL can affect RNA Pol II interactions with chromatin during TCR, we performed FRAP experiments on GFP–RNA Pol II-expressing human fibroblasts depleted or not of ELL. In the presence of ELL, GFP–RNA Pol II mobility is unchanged by UV exposure (Fig. 4*C* and *SI Appendix*, Fig. S9). The absence of any measurable mobility changes or immobile fraction after UV is not surprising for three reasons: (*i*) Most of the FRAP signal is contributed by GFP–RNA Pol II proteins not blocked by DNA lesions residing on the transcribed strand of active genes, (*ii*) a fraction of lesion-stalled GFP–RNA Pol II proteins may be released from the DNA and diffuse away, or (*iii*) they may simply restart transcribing because lesions are continuously being repaired throughout the FRAP experiment. Despite these factors limiting the detection of lesion-blocked RNA Pol II via FRAP, UV irradiation of ELL-depleted GFP–RNA Pol II-expressing cells induces a significant immobile fraction (Fig. 4*D* and *SI Appendix*, Fig. S9), thus indicating that the absence of ELL retains UV-lesion stalled GFP–RNA Pol II to the chromatin, without affecting repair. Interestingly, using a specialized chromatin immunoprecipitation procedure (18, 26), we found ELL interacting, in a UV-dependent manner, with

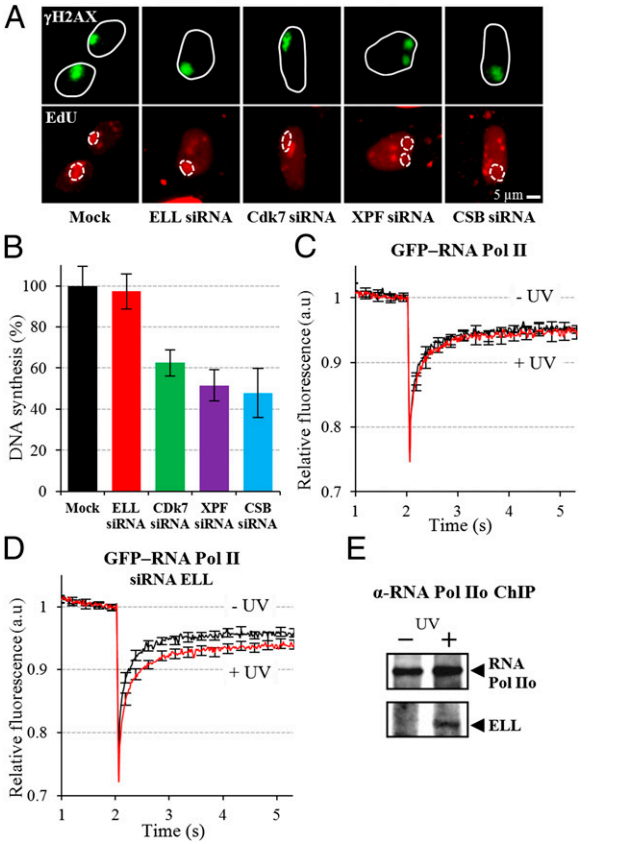

Fig. 4. ELL is essential for resumption of transcription during TCR. (*A*) Confocal images of cells scored for local TCR-UDS. All images were captured using identical settings. (*B*) Quantification of local TCR-UDS in a GGR-deficient cell line treated with siRNA against the indicated factors after local UV irradiation; 50–100 cells were imaged for each case (median ± SEM). (*C*) FRAP curves of RNA Pol II–GFP-expressing cells untreated (black) or treated (red) with UV-C ($n > 30$, mean ± SEM). (*D*) FRAP curves of RNA Pol II–GFP-expressing cells, knocked down for ELL, untreated (black) and treated (red) with UV-C ($n > 30$, mean ± SEM). (*E*) ChIP on protein analysis. Chromatin extracts derived from HeLa cells, 1 h after UV treatment (20 J/m^2) or untreated, were subjected to a RNA Pol IIo-specific ChIP procedure, followed by immunostaining with ELL and RNA Pol IIo antibodies.

chromatin-bound RNA Pol IIo (the elongating form of RNA Pol II) (Fig. 4*E*).

Taken together, our results (RRS, TCR-UDS, FRAP, and ChIP on protein analysis) show that ELL is not implicated in UV-lesion repair per se but is specifically required for efficient RNA Pol II restart upon lesion repair.

Discussion

Although ELL has essentially been associated with complexes with distinct functional activities (4, 6, 7) such as the SEC and the LEC, we have investigated the role of ELL in connection with the general transcription factor TFIIH, in a DNA repair context. Indeed our proteomic analysis revealed, among a set of other potential TFIIH partners, all four LEC components, including ELL.

In this work, we describe ELL as a previously unidentified partner of TFIIH, specifically interacting with the CAK subcomplex via Cdk7. Using several cellular approaches, we have shown that ELL and Cdk7 play essential yet distinct roles during TCR. Whereas absence of the Cdk7 kinase was found to affect UV-lesion repair by TCR, ELL's implication during TCR was not repair-related but seemed crucial to ensure efficient RNA Pol II transcription resumption after lesion repair. Moreover, reduced ELL expression in living cells increased RNA Pol II retention to the chromatin in a UV-dependent manner.

These results logically led us to hypothesize a mechanistic scenario for transcription restart after repair, in which ELL plays a critical role (Fig. 5). In brief, UV-induced lesions blocking RNA Pol II progression will be processed by the TCR machinery. The specific presence of the CAK subcomplex (within TFIIH) during TCR (3) will allow the recruitment of ELL via its interaction with Cdk7. ELL may then serve as a docking site for other proteins needed to stimulate RNA Pol II restart after repair is completed. Clearly, further investigations will be needed to refine the mechanistic details of transcription resumption after UV-lesion repair.

The discovery of ELL as a specific TFIIH interactor recruited during the DNA damage response represents an important step forward in improving our understanding of the largely unknown postrepair transcription restart process. Additionally, finding a direct interaction between a transcription initiation complex (TFIIH) and an elongation factor (ELL) suggests that, in certain cellular circumstances, cross-talk is to be expected between these two processes (27), which could share some of their protein machineries. To conclude, on the basis of this newly discovered ELL function, we propose that in leukemia cells in which ELL is a translocation partner of mixed lineage leukemia (6, 28–30), a defect in transcription resumption after DNA repair could be present. If confirmed, this assumption may lead to new therapeutic strategies for these kinds of leukemias, which are particularly relapsing and require aggressive treatments.

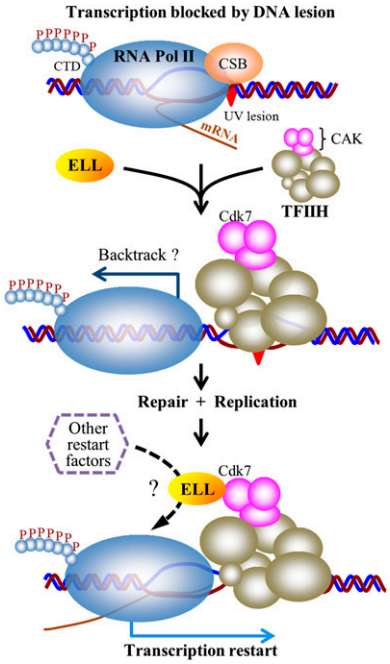

Fig. 5. Mechanistic model of ELL's role in transcription restart after DNA repair. During TCR, ELL can be recruited to the site of damage via its interaction with Cdk7. After completion of the repair reaction (lesion removal and DNA gap filling), ELL plays an essential role to enable RNA Pol II restart, for example as a docking protein to recruit additional factors needed for transcription resumption.

Materials and Methods

Construction and Stable Expression of ELL–GFP Fusion Protein. Full-length ELL cDNA was cloned in-frame into pEGFP-N1 vector (Clontech). Construct was sequenced before transfection. Transfection in MRC5-SV40 transformed human fibroblasts was performed using Fugene transfection reagent (Roche). Stably expressing cells were isolated after selection with G418 (Gibco) and single-cell sorting using FACS (FACScalibur).

Cell Culture and Specific Treatments. Cell strains used were (*i*) XPB–YFP-expressing ES cells (9), (*ii*) wild-type ES cells (IB10), (*iii*) wild-type SV40-immortalized human fibroblasts (MRC5) stably expressing ELL–GFP, (*iv*) MRC5 stably expressing Cdk7–GFP; (*v*) MRC5 transiently expressing RNA Pol II–GFP (31), (*vi*) XPB-deficient SV40-immortalized human fibroblasts (XPCS2BA) stably expressing XPB–GFP, (*vii*) XPC deficient SV40-immortalized human fibroblasts (XP4PA), and (*viii*) Ligase IV null human colon carcinoma cells (HCT-116) (32). ES cell lines were cultured in Buffalo rat liver-conditioned medium supplemented with 1,000 U/mL leukemia inhibitor factor. Human fibroblasts were cultured in a 1:1 mixture of Ham's F-10 and DMEM (Lonza) supplemented with antibiotics and 10% (vol/vol) FCS, at 37 °C, 20% O_2, and 5% CO_2. DNA damage was inflicted by UV-C light (254 nm, 6-W lamp). For UV survival experiments, cells were exposed to different UV-C doses, 1 d after plating. Survival was determined by clone counting 10 d after UV irradiation, as described previously (33). Counting of clones was normalized to the nonirradiated condition for each cell line; this point represents the 100% value in the graph. For FRAP, RRS, and UDS experiments, cells were either globally irradiated with 16 J/m^2 of UV-C or locally irradiated with 30 or 100 J/m^2 of UV-C through a 5-μm-pore polycarbonate membrane filter (Millipore).

Immunoprecipitations, Western Blot, and Mass Spectrometry Analysis. TFIIH immunoprecipitations from whole-cell extracts of wild-type (IB10, for the mock) and XPB–YFP-expressing ES cells were prepared and analyzed by mass spectroscopy as previously described (10). Detailed procedures can be found in *SI Appendix*.

GST Pulldown. GST or GST–ELL polypeptides were expressed in *Escherichia coli* and incubated with glutathione agarose beads. The various subunits of the core TFIIH were expressed in *E. coli* (1×10^6 cells), and cell lysates were incubated with 5 μg of GST or GST-ELL proteins bound to beads at 4 °C for 1 h. Pulldowns were analyzed by Western blotting.

FRAP. FRAP experiments were performed as described in refs. 12 and 13 on a Zeiss LSM 710 NLO confocal laser scanning microscope (Zeiss), using a 40×/1.3 oil objective, under a controlled environment (37 °C and 5% CO_2). Details of the procedure can be found in *SI Appendix*.

Laser Microirradiation. To locally induce DNA damage in living cells, we used a near-infrared laser (Cameleon Vision II; Coherent Inc.) directly coupled to the same LSM 710 NLO (Zeiss). Typically, a small circular area (3 μm in diameter) within the nucleus of a living cell was targeted for ∼35 ms (800 nm, 25% output). Subsequent time-lapse imaging of targeted cells was performed every 15 s for 345 s (488 nm, 1% output). Image analysis was performed using ImageJ (National Institutes of Health) and a custom-built macro as follows: (*i*) The time series image stack was adjusted to compensate for cell movement (StackReg plugin), (*ii*) a region of interest (ROI) spanning the total nucleus was defined to compensate for unwanted photobleaching during the acquisition of images, and (*iii*) a "local damage" ROI was specified to quantify the fluorescence increase owing to (GFP-tagged) protein recruitment at the laser-induced DNA damage area. At least 10 cells were measured for each time point.

RNA Interference. siRNAs used in this study are (*i*) ELL (Sc-38041; Santa Cruz), (*ii*) Cdk7 (L-003241-00-0005; Dharmacon), (*iii*) XPF (M-019946-00; Dharmacon), (*iv*) CSB (pool of two sequences: UGAAGCAUCAGGCUUCGAAdTdT and AGAGAAACGUCUGAA-GCUGdTdT), (*v*) EAF1 (L-019284-01; Dharmacon), (*vi*) KIAA0947 (L-024272-02; Dharmacon), (*vii*) NARG2 (L-014387-00; Dharmacon), and (*viii*) noncoding siRNA (SR-CL000-005; Eurogentec). Cells were transfected using GenJET siRNA transfection reagent (Tebu-Bio) according to the manufacturer's protocol. Transfection complexes were formed by 15-min incubation at room temperature using buffer provided. Briefly, 100,000 cells were seeded per 3-cm dish and allowed to attach overnight. siRNAs were added 24 h (5 nM for ELL, EAF1, KIAA0947, and NARG2; 10 nM for Cdk7, XPF, and CSB) after seeding, and cells were grown confluent. Experiments were carried out 24 or 48 h after seeding. Protein knockdown was confirmed by quantitative RT-PCR.

Quantitative RT-PCR. Total RNA was isolated from siRNA-transfected cells using RNEasy mini kit (Qiagen). cDNA was synthetized using random hexamer primers and SuperScript II Reverse Transcriptase (Invitrogen). ELL, Cdk7, XPF, CSB, EAF1, KIAA0947, and NARG2 expression levels were analyzed using RT-quantitative PCR with the SyberGreen Gene expression assay, using a 7300 real-time PCR machine (Applied Biosystems). ELL, Cdk7, XPF, CSB, EAF1, KIAA0947, and NARG2 expression levels were normalized to HPRT expression.

RRS and UDS Assays. MRC5-SV40 cells were grown on 24-mm coverslips. siRNA transfections were performed 24 h before RRS assays and UDS assays. Procedures for these assays are described in detail in *SI Appendix*.

TCR-UDS Assays: UDS Measurement During TCR. XPC-deficient SV40-immortalized human fibroblasts (XP4PA–GGR-deficient cell line) were grown on 24-mm coverslips. siRNA transfections were performed 24 h before UDS assays. After local irradiation (100 J/m^2 UV-C) through a 5-μm-pore polycarbonate membrane filter (34) cells were incubated for 8 h with 5-ethynyl-2′-deoxyuridine (EdU), washed, fixed, and permeabilized. Fixed cells were treated with a PBS-blocking solution (PBS+: PBS containing 0.15% glycine and 0.5% BSA) for 30 min, subsequently incubated with primary antibodies mouse monoclonal anti–γ-H2AX (Ser139) (clone JBW301; Upstate) 1/500 diluted in PBS+ for 1 h, followed by extensive washes with Tween-20 in PBS. Cells were then incubated for 1 h with secondary antibodies conjugated with Alexa Fluor 488 fluorescent dyes (Molecular Probes; 1:400 dilution in PBS+). Then, cells were incubated for 30 min with the Click-iT reaction mixture containing Alexa Fluor Azide 594. After washing, the coverslips were mounted with Vectashield (Vector). Images of the cells were obtained with the same microscopy system and constant acquisition parameters. Images were analyzed using ImageJ as follows: (*i*) An ROI outlining the locally damaged area was defined by using γ-H2AX staining, (*ii*) a second ROI of comparable size was defined in the nucleus (avoiding nucleoli and other nonspecific signals) to estimate background signal, and (*iii*) the "local damage" ROI was then used to measure the average fluorescence correlated to the EdU incorporation, which is an estimate of DNA replication after repair once the nuclear background signal obtained during step *ii* is subtracted. For each sample, between 90 and 100 nuclei were analyzed from three independent experiments, except for CSB siRNA-treated cells (50 cells from two experiments).

In Vivo Cross-Linking and Chromatin Immunoprecipitation. After UV irradiation (20 J/m^2), cells were cultured for 1 h before cross-linking. In vivo cross-linking was performed as described before (35) with minor modifications. A detailed procedure is described in *SI Appendix*.

ACKNOWLEDGMENTS. Ligase IV null cells were a kind gift of Dr. E. A. Hendrickson (University of Minnesota Medical School, Minneapolis, MN). This work was supported by Action Thématique et Incitative sur Programme Institut National du Cancer/Centre National de la Recherche Scientifique (CNRS) Contract 039438 (to P.-O.M. and G.G.-M.), Region Midi Pyrénées Contract 08017067 (to S.M.), Agence National de la Recherche (ANR) French TFIIH Network (FRET NET) Grant ANR10-BLAN-1231-01 (to S.M. and A.L.), and Recherche Innovation Thérapeutic Cancérologie (A.M.). This work also benefited from the Toulouse Reseau Imagerie (TRI)-RIO Optical Imaging Platform at Institut de Pharmacologie et Biologie Structurale (Genotoul, Toulouse, France) supported by grants from the Région Midi-Pyrénées (contrat de projets état-région), the Grand Toulouse community, the Association pour la Recherche sur le Cancer (Equipement 8505), the CNRS and the European Union through the Fonds Européen de Développement Régional program.

1. Lehmann AR (2003) DNA repair-deficient diseases, xeroderma pigmentosum, Cockayne syndrome and trichothiodystrophy. *Biochimie* 85(11):1101–1111.
2. Hanawalt PC (2002) Subpathways of nucleotide excision repair and their regulation. *Oncogene* 21(58):8949–8956.
3. Coin F, et al. (2008) Nucleotide excision repair driven by the dissociation of CAK from TFIIH. *Mol Cell* 31(1):9–20.
4. Smith ER, et al. (2011) The little elongation complex regulates small nuclear RNA transcription. *Mol Cell* 44(6):954–965.
5. Shilatifard A, Lane WS, Jackson KW, Conaway RC, Conaway JW (1996) An RNA polymerase II elongation factor encoded by the human ELL gene. *Science* 271(5257): 1873–1876.
6. Lin C, et al. (2010) AFF4, a component of the ELL/P-TEFb elongation complex and a shared subunit of MLL chimeras, can link transcription elongation to leukemia. *Mol Cell* 37(3):429–437.
7. Mohan M, Lin C, Guest E, Shilatifard A (2010) Licensed to elongate: A molecular mechanism for MLL-based leukaemogenesis. *Nat Rev Cancer* 10(10):721–728.
8. Luo Z, et al. (2012) The super elongation complex family of RNA polymerase II elongation factors: Gene target specificity and transcriptional output. *Mol Cell Biol* 32(13):2608–2617.
9. Giglia-Mari G, et al. (2009) Differentiation driven changes in the dynamic organization of Basal transcription initiation. *PLoS Biol* 7(10):e1000220.
10. Gautier, V., et al. (2012) Label-free quantification and shotgun analysis of complex proteomes by 1D SDS-PAGE/nanoLC-MS: Evaluation for the large-scale analysis of inflammatory human endothelial cells *Mol Cell Proteomics* 11(8):527–539.
11. Ito S, et al. (2007) XPG stabilizes TFIIH, allowing transactivation of nuclear receptors: Implications for Cockayne syndrome in XP-G/CS patients. *Mol Cell* 26(2):231–243.
12. Giglia-Mari G, et al. (2006) Dynamic interaction of TTDA with TFIIH is stabilized by nucleotide excision repair in living cells. *PLoS Biol* 4(6):e156.
13. Hoogstraten D, et al. (2002) Rapid switching of TFIIH between RNA polymerase I and II transcription and DNA repair in vivo. *Mol Cell* 10(5):1163–1174.
14. Vermeulen W (2011) Dynamics of mammalian NER proteins. *DNA Repair (Amst)* 10(7): 760–771.
15. van Royen ME, Zotter A, Ibrahim SM, Geverts B, Houtsmuller AB (2011) Nuclear proteins: Finding and binding target sites in chromatin. *Chromosome Res* 19(1):83–98.
16. Svejstrup JQ, et al. (1995) Different forms of TFIIH for transcription and DNA repair: Holo-TFIIH and a nucleotide excision repairosome. *Cell* 80(1):21–28.
17. Godon C, et al. (2012) Generation of DNA single-strand displacement by compromised nucleotide excision repair. *EMBO J* 31(17):3550–3563.
18. Fousteri M, Vermeulen W, van Zeeland AA, Mullenders LH (2006) Cockayne syndrome A and B proteins differentially regulate recruitment of chromatin remodeling and repair factors to stalled RNA polymerase II in vivo. *Mol Cell* 23(4):471–482.
19. Meldrum RA, Botchway SW, Wharton CW, Hirst GJ (2003) Nanoscale spatial induction of ultraviolet photoproducts in cellular DNA by three-photon near-infrared absorption. *EMBO Rep* 4(12):1144–1149.
20. Politi A, et al. (2005) Mathematical modeling of nucleotide excision repair reveals efficiency of sequential assembly strategies. *Mol Cell* 19(5):679–690.
21. Roy R, et al. (1994) The MO15 cell cycle kinase is associated with the TFIIH transcription-DNA repair factor. *Cell* 79(6):1093–1101.
22. Limsirichaikul S, et al. (2009) A rapid non-radioactive technique for measurement of repair synthesis in primary human fibroblasts by incorporation of ethynyl deoxyuridine (EdU). *Nucleic Acids Res* 37(4):e31.
23. Mu D, Hsu DS, Sancar A (1996) Reaction mechanism of human DNA repair excision nuclease. *J Biol Chem* 271(14):8285–8294.
24. Matsumoto M, et al. (2007) Perturbed gap-filling synthesis in nucleotide excision repair causes histone H2AX phosphorylation in human quiescent cells. *J Cell Sci* 120(Pt 6): 1104–1112.
25. Vrouwe MG, Pines A, Overmeer RM, Hanada K, Mullenders LH (2011) UV-induced photolesions elicit ATR-kinase-dependent signaling in non-cycling cells through nucleotide excision repair-dependent and -independent pathways. *J Cell Sci* 124(Pt 3): 435–446.
26. Fousteri M, Mullenders LH (2008) Transcription-coupled nucleotide excision repair in mammalian cells: Molecular mechanisms and biological effects. *Cell Res* 18(1):73–84.
27. Larochelle, S., et al. (2012) Cyclin-dependent kinase control of the initiation-to-elongation switch of RNA polymerase II. *Nat Struct Mol Biol* 19(11):1108–1115.
28. Mueller D, et al. (2009) Misguided transcriptional elongation causes mixed lineage leukemia. *PLoS Biol* 7(11):e1000249.
29. Bitoun E, Oliver PL, Davies KE (2007) The mixed-lineage leukemia fusion partner AF4 stimulates RNA polymerase II transcriptional elongation and mediates coordinated chromatin remodeling. *Hum Mol Genet* 16(1):92–106.
30. Smith E, Lin C, Shilatifard A (2011) The super elongation complex (SEC) and MLL in development and disease. *Genes Dev* 25(7):661–672.
31. Mari PO, et al. (2010) Influence of the live cell DNA marker DRAQ5 on chromatin-associated processes. *DNA Repair (Amst)* 9(7):848–855.
32. Fattah F, et al. (2010) Ku regulates the non-homologous end joining pathway choice of DNA double-strand break repair in human somatic cells. *PLoS Genet* 6(2):e1000855.
33. Jensen A, Mullenders LH (2010) Transcription factor IIS impacts UV-inhibited transcription. *DNA Repair (Amst)* 9(11):1142–1150.
34. Moné MJ, et al. (2001) Local UV-induced DNA damage in cell nuclei results in local transcription inhibition. *EMBO Rep* 2(11):1013–1017.
35. Orlando V, Strutt H, Paro R (1997) Analysis of chromatin structure by in vivo formaldehyde cross-linking. *Methods* 11(2):205–214.